

Annual Performance Report
for the period 15 April 1996 - 14 April 1997

for

NASA Grant No. NAG 5-2927

entitled

EVALUATING AND UNDERSTANDING PARAMETERIZED
CONVECTIVE PROCESSES AND THEIR ROLE IN THE DEVELOPMENT
OF MESOSCALE PRECIPITATION SYSTEMS

submitted to

Ms. Gloria R. Blanchard
Grants Officer
NASA/Goddard Space Flight Center
Code 286.1
Greenbelt, MD 20771

by

J. Michael Fritsch
Principal Investigator
Department of Meteorology

and

John S. Kain
Co-Principal Investigator
Department of Meteorology

The Pennsylvania State University
Office of Sponsored Programs
110 Technology Center
University Park, PA 16802

February 25, 1997

018777

Evaluating and Understanding Parameterized Convective Processes and Their Role in the Development of Mesoscale Precipitation Systems

NASA Grant NAB 5-2927
Second Year (3/1/96 - 2/28/97) Annual Report
John S. Kain, J.M. Fritsch, and Robert F. Rogers
Department of Meteorology
The Pennsylvania State University

I. Summary of Progress

Research efforts during the second year have centered on improving the manner in which convective stabilization is achieved in the Penn State/NCAR mesoscale model MM5 (Grell *et al.*, 1994). Ways of improving this stabilization have been investigated by 1) refining the partitioning between the Kain-Fritsch convective parameterization scheme (Kain and Fritsch, 1993 - KF) and the grid scale by introducing a form of moist convective adjustment; 2) using radar data to define locations of subgrid-scale convection during a dynamic initialization period; and 3) parameterizing deep-convective feedbacks as subgrid-scale sources and sinks of mass. These investigations were conducted by simulating a long-lived convectively-generated mesoscale vortex that occurred during July 14-18 1982 and the June 10-11 1985 squall line that occurred over the Kansas-Oklahoma region during the PRE-STORM experiment. The long-lived vortex tracked across the central Plains states and was responsible for multiple convective outbreaks during its lifetime (Fritsch *et al.*, 1994).

a. Moist convective adjustment

Kain and Fritsch (1997) described a problem that has troubled mesoscale modelers for many years: the development of a moist absolutely unstable structure in the lower troposphere that leads to overturning on the grid scale. In their simulation of the June 10-11 squall line, which compared favorably with observations, the development of the strongest perturbations was consistently preceded by the formation of these moist, absolutely unstable structures. As they pointed out, the development of an absolutely unstable structure in the model does not necessarily simply reflect errors in the model or, more specifically, errors in the KF scheme.

It is quite reasonable to speculate how these structures can appear in nature. For example, deep convective cells can develop in an area and produce evaporatively-cooled downdrafts that typically stabilize the boundary layer and generate a pool of cold air near the surface. As this cold pool propagates outward, it can undercut surrounding air and lift a deep, potentially unstable layer to its saturation point. On larger scales, lifting can be facilitated by a frontal boundary, where, again, a deep layer of potentially unstable air can be lifted to its saturation point (*e.g.*, Trier and Parsons, 1993). Figures 1-3 illustrate how this can occur and how this instability would appear if penetrated by an atmospheric sounding. In particular, Fig. 1a shows a conditionally unstable environment just prior to being lifted by a surface-based cold layer such as that depicted in Fig. 2. With modest ascent rates corresponding to the vertical velocity profile shown in Fig. 3 (and imposed low-level cooling), the conditionally unstable sounding shown in Fig. 1a can be

transformed into the nearly saturated structure shown in Fig. 1b within 3 hours. At this stage, the sounding would be absolutely unstable between about 650 and 500 mb and on the verge of becoming absolutely unstable down to 800 mb. Although this instability rarely appears in soundings derived from radiosonde ascents, its diagnosis is not unprecedented. For example, Fig. 4 shows a sounding taken from Ardmore, OK during VORTEX (Verification of the Origins of Rotation in Tornadoes Experiment). In this sounding the lapse rate in the layer from about 775 mb to about 625 mb is much greater than the moist-adiabatic value and the air is saturated or very nearly so.

Recognizing the possibility that the development of moist absolutely unstable layers may be physically reasonable, it becomes important to understand how this structure develops in the model, and how it is alleviated by the model. The KF convective scheme can only process one 50-100 mb layer at a time during a given convective time period, which ranges between 30 minutes and an hour. However, given sufficiently high relative humidities and vertical motions, the saturation process can take place over layers deeper than 100 mb and over a time scale comparable to a convective time scale. Therefore, the parameterization scheme is incapable of stabilizing the deep moist layer, and it becomes absolutely unstable. In fact, often the resolvable-scale overturning occurs while the convective scheme is still active, so that the overturning is represented partly as a parameterized, subgrid-scale process, and partly as a hydrostatic manifestation of convective overturning.

The problem with this representation is that often the heating and moistening tendencies and their resulting mesoscale signatures are overestimated, depending on which layers become absolutely unstable and on what the magnitude of the resulting overturning is. This suggests that the realism of the model depiction of this instability is limited by the manner in which the overturning is achieved; namely, the partial depiction of the overturning occurring hydrostatically, with time scales on the order of several hours. By weakening the magnitude of this hydrostatic overturning, the diabatic effects of the convection can be brought more into line with expectations. To accomplish this, we have envisioned the overturning of saturated absolutely unstable layers as a moist convective mixing process similar to the dry convective adjustment that occurs when a superadiabatic layer forms at the surface during daytime heating. In that case, incoming shortwave radiation is strong enough to warm the surface such that the heat flux to the air creates a lapse rate that is steeper than dry adiabatic. As that occurs, the atmosphere is quickly rearranging mass to maintain a dry adiabatic profile with a form of rapid mixing within all layers of the boundary layer. In this situation, the dissipation of the instability from buoyantly-generated eddies rising from the surface represents the dry convective adjustment needed to minimize the instability created from the surface heat flux. For the case of moist convective adjustment, the instability is created and maintained by the presence of large-scale upward motion (such as what occurs over an outflow boundary or a frontal boundary). Convective clouds are initiated, but they are insufficient to alleviate the moist absolute instability when it occurs over a large depth. Therefore, mixing similar to what was described above occurs, except that it tends to adjust the atmosphere toward a moist adiabatic profile instead of a dry adiabatic lapse rate. Of course, once moisture is considered with its associated phase changes, the need to conserve energy demands a scheme that can account for these various phases.

With the above considerations in mind, we constructed a hybrid convective parameterization procedure which uses two different routines to introduce the effects of both penetrative convective towers and the moist mixing that locally drives the thermodynamic profile

towards moist adiabatic conditions. The KF scheme was employed to introduce the effects of the deep convective towers and the Betts-Miller convective scheme (Betts, 1986 - BM) was employed to accomplish the moist mixing. Note, however, that this hybrid scheme was only initiated at grid points where the KF scheme was active and a saturated layer with a lapse rate steeper than moist adiabatic formed.

Tests of the hybrid scheme were conducted by simulating the long-lived mesovortex of July 14-18 1982 described by Fritsch *et al.* (1994). For these simulations, the fine-mesh resolution was 18 km, and the Blackadar high-resolution boundary layer formulation (Zhang *et al.*, 1982) and ice phase microphysics were included.

The impacts of this modification became quite evident as the model developed widespread parameterized convection. By 15 hours of simulation time, parameterized convection was widespread over eastern Nebraska and southeastern South Dakota in both runs. For the run without the hybrid procedure, sea level pressures lowered in this region, with a 2-3 mb mesolow over northeast Nebraska (Fig. 5). This does not agree with observations, which show that pressures were higher over southeastern South Dakota associated with a mesoscale convective complex there. Comparing this run with a run that uses the hybrid procedure shows that the mesolow has been replaced by a weak mesohigh over a broad region (Fig. 6). Surface winds also show an anticyclonic perturbation in the region of the mesohigh in the run with the hybrid procedure. In general, when this adjustment is allowed the surface features seem much more reasonable and they resemble features that are typically observed with mesoscale convective systems (*e.g.*, mesohigh, anticyclonically perturbed winds).

Cross sections of the various convective heating terms illustrate the reasons for the differences between the two runs. Figures 7a and 7b show cross sections of KF scheme convective heating and grid-resolved heating, respectively, for the run without the hybrid procedure. Maximum heating rates from the KF scheme are about 3-4 K hr⁻¹ between 300 and 400 mb, while heating rates from explicitly-resolved processes are considerably greater, with values larger than 80 K hr⁻¹ appearing between 600 and 400 mb. This heating is the model-resolved manifestation of a thermal rising within the column with horizontal dimensions larger than the model resolution of 18 km. The response to this heating is an intense warm core in the middle and upper troposphere and a subsequent hydrostatic lowering of pressure at the surface, appearing as the mesolow in Fig. 5. Figures 8a, b, and c show cross sections of KF scheme convective heating, grid-scale heating, and BM scheme convective heating, respectively, for the run with the hybrid procedure. The KF heating is of the same magnitude as Fig. 7a, with maximum heating rates of 5 K hr⁻¹ around 400 mb. Grid-scale convective heating is much smaller than the run without moist convective adjustment, with values limited to 12 K hr⁻¹ in the mid troposphere. The moist convective adjustment represented by the BM scheme appears as convective heating on the order of 10 K hr⁻¹ (Fig. 8c). This heating represents the rearranging of mass that is necessary to bring the atmosphere back into a moist convectively neutral state. Conceptually it is similar to the heating that occurs in a convective boundary layer as thermals originate at the surface and rise to the top of the boundary layer, warming the boundary layer during their ascent. While some of the heating is still accomplished by the grid scale, it is much smaller than the run without this adjustment (*cf.* Figs. 8b and 7b). The result of this diminished grid-scale heating is a weaker midlevel warm core and a mesohigh at the surface instead of a mesolow.

These results are encouraging in demonstrating the ability of this technique to dampen the heating that occurs on the grid scale when moist absolutely unstable structures occur in the model while retaining the important effects of the deep convective towers (*e.g.*, penetrative moist downdrafts). Clearly it is impossible to quantify exactly how much dampening should occur, especially as different cases are simulated and different model resolutions are employed. The most readily-available means of gauging the success of this approach is by comparing these runs against measurable quantities, such as sea-level pressure and observed rainfall. More work needs to be done in both the theoretical and modeling realm to gain a more solid foundation upon which to base this technique.

b. Radar nudging

Much energy has been exerted in developing convective parameterizations that realistically reflect the effects of convection on resolvable-scale fields. However, comparatively little attention has been given to developing criteria for determining when and where deep convection will occur. When and where parameterized convection occurs in a given model simulation influences the vertical distribution of heating, the propagation of gravity waves from the convection, the movement of outflow boundaries, and many other nonlinear feedbacks that can substantially alter the results of the simulation. Thus it is crucial to be able to accurately diagnose the timing and location of convective initiation.

Despite the recognition of the importance of accurately capturing the timing and placement of convection (Rogers and Fritsch, 1996; Stensrud and Fritsch, 1994; Kain and Fritsch, 1992), MM5 often fails in this regard. This failure can be attributed to many factors: the trigger function may be deficient, the initial conditions may not capture features important for the initiation of parameterized convection, and the boundary layer parameterization may be inadequate, to name a few. In recognition of this problem, radar data has been proposed to be used as a source for initiating and suppressing convection in the model using the KF scheme (Lambert, 1994). The methodology involves digitizing radar data to the model grid at high temporal frequencies (*e.g.*, every fifteen minutes). In regions or times where there is no radar data available, the convective parameterization is allowed to operate independently. If the radar indicates there is no convection present (convection being defined as having a VIP return greater than or equal to 3), the parameterization scheme is not allowed to initiate convection. If the radar indicates there is convection present, and the parameterization is going to initiate convection, then it is allowed to do so. If the parameterization is not going to initiate convection, then convection is forced within the scheme. The source layer chosen for convective forcing is that layer with the highest θ_e value. An artificially large thermal (or vertical velocity, depending on the trigger function) perturbation is imposed on the source layer to ensure that the perturbation will reach its level of free convection. If the cloud depth is less than a specified amount (in this case 4 km), the θ_e of the source layer is increased by adding 0.5 g/kg of water vapor to the layer. If the cloud is still not deep enough, another 0.5 g/kg of water vapor is added. If the cloud is still not deep enough, convection is considered to be not possible, and the grid point is skipped.

We have tested this technique in our simulations of the long-lived mesovortex described above in hopes of more accurately capturing the evolution of convection. As expected, nudging with radar observations for 24 hours produces a highly realistic reproduction of convective distribution, outflow boundary location and magnitude, and surface pressure distribution.

However, several problems also arise when using this technique. The presence of the Rocky mountains in the domain leads to the development of a strong solenoidal circulation during the daytime hours between the mountain ridges and the high plains to the east. However, no convection is observed in the radar data. Therefore, the convective parameterization scheme is prevented from operating. With no mechanism for accomplishing subgrid-scale eddy fluxes of heat and moisture that occur with the convective scheme, the strong circulations in the model saturate the lower troposphere on the grid scale. This establishes a region of absolute instability like what was described in the previous section. Strong grid-scale overturning occurs, and the resulting squall-line-type structure propagates through the domain, even though no convection was observed there. A similar problem occurs in the northern Plains, where the boundary layer is very moist, and weak upward motion associated with the diurnal heating cycle brings the grid scale to saturation. Evidently deficiencies in the simulation, whether in the initialization, boundary condition specification, model physics, or some combination of them, are creating structures that do not occur in nature which are leading to the formation of these absolutely unstable structures. We are currently attempting to rectify the problem of the creation of spurious grid-scale overturning. One option is to force convection where it is observed, but not suppress it where it is not observed. Other tests are being conducted to determine the optimal length of time that radar nudging should be employed.

c. Parameterizing deep-convective feedbacks as subgrid-scale sources and sinks of mass

Mass-flux parameterizations of deep convection use simple cloud models to rearrange unstable distributions of mass in the atmosphere into more stable stratifications. Compared to parameterizations based on empirically-derived reference profiles, mass-flux approaches are appealing because they allow one to envision a physically-based, buoyancy-driven process by which stabilization is achieved. Furthermore, this type of parameterization is potentially useful for diagnosing vertical transports of hydrometeors and other constituents of the air, such as chemical species or inert tracers.

In traditional methods for formulating this type of parameterization, it is assumed that mass continuity can be maintained by forcing the subgrid-scale cloud environment, i.e., the mass within a given grid element, to move vertically in exact compensation for the vertical transports in convective drafts. This assumption has significant implications because the compensatory environmental motions produce the bulk of the parameterized temperature and moisture changes, except in those limited layers where updraft and downdraft detrainment rates are strong. However, the validity of this assumption is questionable. In particular, as model grid-lengths are reduced to the point where explicitly-resolved scales approach the scales of convective clouds it is unlikely that all of the compensation for local convective transports occurs within the same grid element. Thus, alternative formulations are needed.

We have investigated an alternative to the imposition of local compensating subsidence within the framework of the Kain-Fritsch convective parameterization scheme (CPS) and the Penn State/NCAR mesoscale model (MM5). In the new formulation, subgrid-scale convective transports are represented in the nonhydrostatic equations of motion as sources and sinks of mass which are converted to equivalent pressure perturbations. In particular, convective entrainment and detrainment rates are expressed as negative and positive contributions, respectively, to the pressure-perturbation tendency. These contributions are represented in a single additional term

added to the pressure-perturbation (p') tendency equation, expressed in flux form, found in the MM5 model description (Grell *et al*, 1994),

$$\frac{\partial p^* p'}{\partial t} = \left(\text{horizontal advection of } p' + (\text{vertical advection of } p') + (\text{divergence term associated with } p') + (\text{acoustic terms}) + (\text{vertical advection of base state}) + \frac{\partial p^* p'}{\partial t} \right)_c$$

where $\left(\frac{\partial p^* p'}{\partial t} \right)_c$ is the contribution to the pressure perturbation tendency from the convection.

This contribution is represented by the expression

$$\left(\frac{\partial p^* p'}{\partial t} \right)_c = - p^* \gamma p \beta_p$$

where p^* is the surface pressure minus the pressure of the model top, γ is the ratio of heat capacities (c_p/c_v) for dry air, and p is the total pressure at a grid point. The β_p term represents the source or sink of mass due to entrainment or detrainment from convective drafts, *i.e.*,

$$\beta_p = \frac{(\delta_u + \delta_d + \varepsilon_u + \varepsilon_d)}{M},$$

where δ represents detrainment rate and ε represents entrainment rate (both in units of kg s^{-1} , and the subscripts u and d denote updraft and downdraft, respectively. M is the total mass (kg) within the model layer. With this formulation, mass imbalances that are created by the removal or deposition of mass by convective updrafts and downdrafts are "felt" by the full equations of motion and compensating circulations are generated on resolvable scales.

In addition, entrainment (detrainment) of predictive variables (e.g., temperature and moisture) is represented in the variable's tendency equations in a manner analogous to horizontal advection out of (into) the grid-element. For example, with this type of feedback imposed, the flux-form temperature tendency equation in MM5 becomes

$$\frac{\partial p^* T}{\partial t} = \left(\text{horizontal advection } T + (\text{vertical advection of } T) + (\text{divergence term associated with } T, \text{ with the addition of the term } (p^* \beta_p)) + (\text{changes in temperature due to changes in pressure}) + (\text{diabatic terms}) + (\text{diffusion of } T) + \frac{\partial p^* T}{\partial t} \right)_c$$

where $\left(\frac{\partial p^* T}{\partial t} \right)_c$ is the contribution to the temperature tendency from the convection. This contribution is represented by the expression

$$\left. \frac{\partial p^* T}{\partial t} \right)_c = p^* \beta_T$$

where β_T represents the source and sink of *temperature* in a layer due to entrainment or detrainment from convective drafts,

$$\beta_T = \frac{(\delta_u T_u + \delta_d T_d + (\varepsilon_u + \varepsilon_d) T_{E_o})}{M},$$

and the subscript E_o denotes the value in the convective environment at the time convection is initiated. This value is appropriate because convection is assumed to remain active in a steady-state for multiple model time steps.

This concept was tested using MM5 for a simulation of the June 10-11 1985 squall line. This system has been studied extensively and simulated with numerous different configurations of MM5 (Zhang *et al.* 1989; Wang *et al.* 1996; Kain and Fritsch 1997). For these runs, a 25 km grid length was used and ice-phase microphysics were included. Some results from the 18 h time of this experimental simulation, corresponding to the mature stage of the squall line, are shown in Fig. 9. For comparison, corresponding results from a control simulation with identical model configuration, except for the modifications indicated above, are shown in Fig. 10.

The position of the outflow boundary corresponding to the leading edge of the squall line is similar in the two simulations, but the structure of the surface pressure field is quite different (cf. Figs. 9a and 10a). In particular, the pressure field in the experimental run is much noisier than in the control, especially to the rear of the leading line. In general, it was found that the pressure-perturbation feedbacks generated quite a bit of noise in the pressure field within convectively-active areas throughout this simulation. It can also be seen that the rather intense wake low that appears over south-central Kansas in the control simulation is difficult to discern in the experimental run. As discussed in previous studies (e.g., Zhang *et al.* 1989; Kain 1994), this feature is closely linked to intense grid-scale precipitation rates and tends to form on the back edge of the area of heaviest precipitation. Thus, the position of this feature is consistent with the resolved-scale rainfall pattern shown in Fig. 10b, indicating a maximum rainfall of 4.37 cm during the 17 to 18 h time period just to the east of the center of the wake low. By comparison, the run with the mass source/sink feedbacks also had a grid-scale precipitation maximum in this region, but the magnitude of the maximum value was considerably lower, at about 0.67 cm (Fig. 9b). These differences are indicative of a weaker overall squall line circulation in this region in the experimental run. This trend can also be seen in the one-hour parameterized rainfall totals (cf. Figs. 9c and 10c). The areal coverage of rainfall is about the same in the two runs, but rates are much lower in the experimental run.

In general, the results from this experimental run are consistent with numerous other test runs that were done with the mass source/sink feedback. This alternative type of feedback tended to lead to generate noisier fields of all variables in the vicinity of active convection and it consistently generated weaker convectively-induced circulations. A detailed analysis of these induced circulations indicated that almost all of the response occurred in the vertical, similar to what is imposed in the traditional method of computing compensating subsidence rates to offset

convective fluxes. The fact that most of the direct response was confined to the convecting column is consistent with the magnitude of the pressure gradients that were created. In particular, with a 25 km horizontal grid length and a vertical spacing on the order of 1 km, the pressure-perturbation *gradient* that induces the response was much stronger in the vertical.

It is also important to note that the character of the response with this type of feedback is quite different from the traditional approach. In the traditional approach, heating is assumed to occur within the cloud layer primarily as a consequence of downward moving subgrid-scale air in the convective environment (i.e., the "compensating subsidence" effect). This heating is then fed back as if it were an external heat source. The natural response to this heating is upward motion on resolved scales. As discussed by Kain and Fritsch (1997) this upward motion continues until the heating is approximately eliminated. Not coincidentally, the grid-scale mass flux required to just about eliminate the warm anomaly is approximately equal and opposite to the downward flux of mass (i.e., the "compensating subsidence") that created the heating. Thus, the net vertical mass flux (i.e., the sum of the computed subgrid-scale compensating subsidence and the grid-scale response) is approximately zero, but typically the only vertical motion seen within the cloud layer on the model grid is upward.

With the mass source/sink type of feedback, parameterized forcing does not heat the column right away. Instead, it induces a positive pressure perturbation due to updraft detrainment aloft and a negative pressure perturbation in the sub-cloud layer, where mass is being evacuated to feed the updraft. Thus, the top to bottom perturbation-pressure gradient induces downward motion at that grid point. However, as the sinking air begins to warm, it creates a positive local temperature anomaly, and by hydrostatic considerations a corresponding local height anomaly, which, by itself, would induce upward motion locally. The vertical motion computed at a convectively-active grid point reflects the net dynamical effect of these two perturbations, and is typically characterized by strong sinking motion at most model layers within the parameterized-cloud layer for the first one-half to three-quarters of the convective cycle, followed by a gradual switch over to upward motion. The upward motion continues, as with the traditional feedback, until the local mass-field anomalies are approximately eliminated.

In general we are quite encouraged by these results and we feel that the mass source/sink type of feedback may be a viable alternative to traditional methods requiring local imposition of compensating subsidence.

II. Work Plan: March 1, 1997 - February 28, 1998

In light of the fact that Jack Kain has moved to NSSL and Robert Rogers has taken his place, we have modified the work plan for the upcoming year to exploit Rogers' expertise while continuing to address the pertinent issues as outlined in the original work plan.

A. Investigate methods for improving the performance of convective parameterization schemes

Our work with the MM5 modeling system has shown that deep convection is often represented by both parameterized and explicitly-resolved processes. In some instances, the representation of convective overturning on the grid scale results in features that are too strong, as compared with observations. In the upcoming year methods for improving the feedbacks that

result from the parameterized convective schemes (namely, the KF scheme) will be pursued. These efforts will include further diagnostic studies of the hybrid scheme described above and the use of radar data to place parameterized convection in the model.

The applicability of these techniques to simulations of systems over tropical waters will be tested by inserting a warm water body underneath the long-lived convectively-generated mesoscale vortex described above. This modification will replicate conditions that are typically observed over the tropical oceans and will provide an opportunity to determine the potential benefits of using a hybrid convective scheme and radar data during a dynamic initialization in this environment.

III. Travel supported by this grant during 1996

Dr. John S. Kain was partially supported by this grant, in an amount of \$885.00, for travel to Seon, Bavaria, Germany to attend the NATO Advanced Study Institute on The Physics and Parameterization of Moist Atmospheric Convection. This Institute took place between August 5 and 16, 1996. This meeting gave Dr. Kain a rare opportunity to interact with many of the world's leading experts on convection and convective parameterization and to present scientific results to this group in a talk entitled "Parameterizing Convective Forcing in Mesoscale Models". His interactions with this group of scientists were mutually beneficial as he gained additional insight into the convective parameterization problem as a result of their expertise, while at the same time impressing upon them the necessity of practicable approaches to addressing this problem. Dr. Kain's travel to this Institute will benefit NASA because his contributions to the grant will be enhanced by the insight he has gained into the convective parameterization problem and because his interactions at this particular meeting will facilitate future collaborations with the international community.

IV. Publications during 1996

Kain, J.S., and J.M. Fritsch, 1997: Multiscale Convective Overturning in Mesoscale Convective Systems: Reconciling Observations, Simulations, and Theory. Submitted to *Monthly Weather Review*.

Kuo, Y.-H., J. Bresch, M.-D. Cheng, J.S. Kain, D.B. Parsons, W.-K. Tao, and D.-L. Zhang, 1996: Summary of a Mini-Workshop on Cumulus Parameterization for Mesoscale Models. *Bulletin of the American Meteorological Society*, in press.

Wang, Y., W.-K. Tao, K.E. Pickering, A.M. Thompson, J.S. Kain, R.F. Adler, J. Simpson, P.R. Keehn, and G.S. Lai, 1996: Mesoscale model simulations of TRACE-A and PRE-STORM convective systems and associated tracer transport. *Journal of Geophysical Research*, TRACE A and SAFARI special issue, 24013-24028.

References

- Betts, A.K., 1986: A new convective adjustment scheme. Part I. Observational and theoretical basis. *Quart. J. Roy. Meteor. Soc.*, **112**, 677-691.
- Fritsch, J.M., J.D. Murphy, and J.S. Kain, 1994: Warm core vortex amplification over land. *J. Atmos. Sci.*, **51**, 1780-1807.
- Grell, G.A., J. Dudhia, and D.R. Stauffer, 1994: A description of the fifth generation Penn State/NCAR mesoscale model (MM5). NCAR Tech Note, NCAR/TN-398+STR, 138 pp.
- Kain, J.S., 1994: Interactions between parameterized convection and grid-scale circulations in a mesoscale model. Ph.D. Dissertation, Pennsylvania State University, 143 pp.
- Kain, J.S., and J.M. Fritsch, 1992: The role of the convective "trigger function" in numerical forecasts of mesoscale convective systems. *Meteorol. Atmos. Phys.*, **49**, 93-106.
- Kain, J.S., and J.M. Fritsch, 1993: Convective parameterization for mesoscale models: The Kain Fritsch scheme. *The representation of cumulus convection in numerical models. Meteor. Monogr.*, No. 24, Amer. Meteor. Soc., 165-170.
- Kain, J.S., and J.M. Fritsch, 1997: Multiscale Convective Overturning in Mesoscale Convective Systems: Reconciling Observations, Simulations, and Theory. Submitted to *Monthly Weather Review*.
- Lambert, W., 1994: A procedure for using radar reflectivity data to locate convection in the dynamic initialization of a mesoscale model. M.S. Thesis, The Pennsylvania State University, 95 pp.
- Rogers, R.F., and J.M. Fritsch, 1996: A general framework for convective trigger functions. *Mon. Wea. Rev.*, **124**, 2438-2452.
- Stensrud, D.J., and J.M. Fritsch, 1994: Mesoscale convective systems in weakly forced large-scale environments. Part III: Numerical simulations and implications for operational forecasting. *Mon. Wea. Rev.*, **122**, 2084-2104.
- Trier, S.B., and D.B. Parsons, 1993: Evolution of environmental conditions preceding the development of a nocturnal mesoscale convective complex. *Mon. Wea. Rev.*, **121**, 1078-1098.
- Wang, Y., W.-K. Tao, K.E. Pickering, A.M. Thompson, J.S. Kain, R.F. Adler, J. Simpson, P.R. Keehn, and G.S. Lai, 1996: Mesoscale model simulations of TRACE-A and PRE-STORM convective systems and associated tracer transport. *Journal of Geophysical Research*, TRACE A and SAFARI special issue, 24013-24028.

- Zhang, D.-L., and R.A. Anthes, 1982: A high-resolution model of the planetary boundary layer-- Sensitivity tests and comparisons with SESAME-79 data. *J. Appl. Meteor.*, **21**, 1594-1609.
- Zhang, D.-L., K. Gao, and D.B. Parsons, 1989: Numerical simulation of an intense squall line during 10-11 June 1985 PRE-STORM. Part I: Model verification. *Mon. Wea. Rev.*, **117**, 960-994.

Figure Captions:

- Fig. 1. a) A conditionally unstable vertical sounding typical of a preconvective environment over the Great Plains of the U.S., shown on a Skew-T log-P diagram; b) the same environment after 3 h of lifting at the rate indicated by Fig. 3 and with imposed low-level cooling (from Kain and Fritsch, 1997)
- Fig. 2. Conceptual diagram of a low-level jet of warm, moist air overrunning the relatively cool low-level air north of a warm front (from Trier and Parsons, 1993)
- Fig. 3. Vertical profile of vertical motion ($\mu\text{b s}^{-1}$) used to calculate the effects of forced ascent on the sounding shown in Fig. 1a (from Kain and Fritsch, 1997)
- Fig. 4. Vertical sounding derived from radiosonde measurements from Ardmore, OK, valid 2315 UTC 19 April 1995 and plotted on a Skew-T log-P diagram (from Kain and Fritsch, 1997)
- Fig. 5. Sea level pressure (mb) and lowest sigma-level ($\sigma = 0.997$) winds (max vector = 13.5 m s^{-1}) at 15 h for simulation without hybrid procedure. Location of cross sections appearing in Fig. 6 is indicated by line AB.
- Fig. 6. As in Fig. 5, but for simulation with hybrid procedure. Location of cross sections appearing in Fig. 6 is indicated by line CD.
- Fig. 7. Cross sections of convective heating at 15 hours for simulation without hybrid procedure from a) KF convective scheme (K hr^{-1} , contour interval 1 K hr^{-1}); b) grid scale (K hr^{-1} , contour interval 3 K hr^{-1})
- Fig. 8. Cross sections of convective heating at 15 hours for simulation with hybrid procedure from a) KF convective scheme (K hr^{-1} , contour interval 1 K hr^{-1}); b) grid scale (K hr^{-1} , contour interval 3 K hr^{-1}); and BM scheme (K hr^{-1} , contour interval 1 K hr^{-1})
- Fig. 9. Results from the 18 h time period from a simulation using the mass source/sink type of feedback in the KF scheme: a.) Sea-level pressure (mb), b.) grid-resolved 17 to 18h rainfall (cm), c.) parameterized convective 17 to 18 h rainfall (cm).
- Fig. 10. As in Fig. 1, but for a simulation using the normal feedback method in the KF scheme.

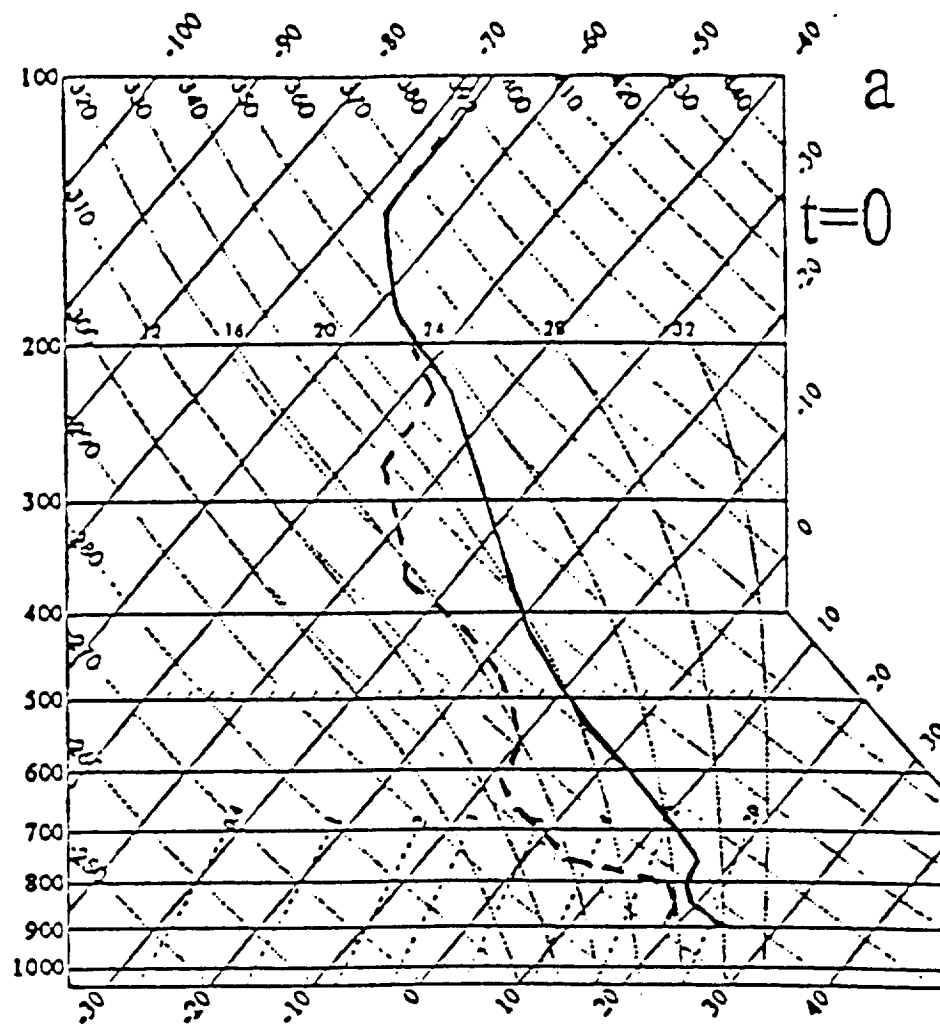


Fig. 1a. A conditionally unstable vertical sounding typical of a preconvective environment over the Great Plains of the U.S., shown on a Skew-T log-P diagram

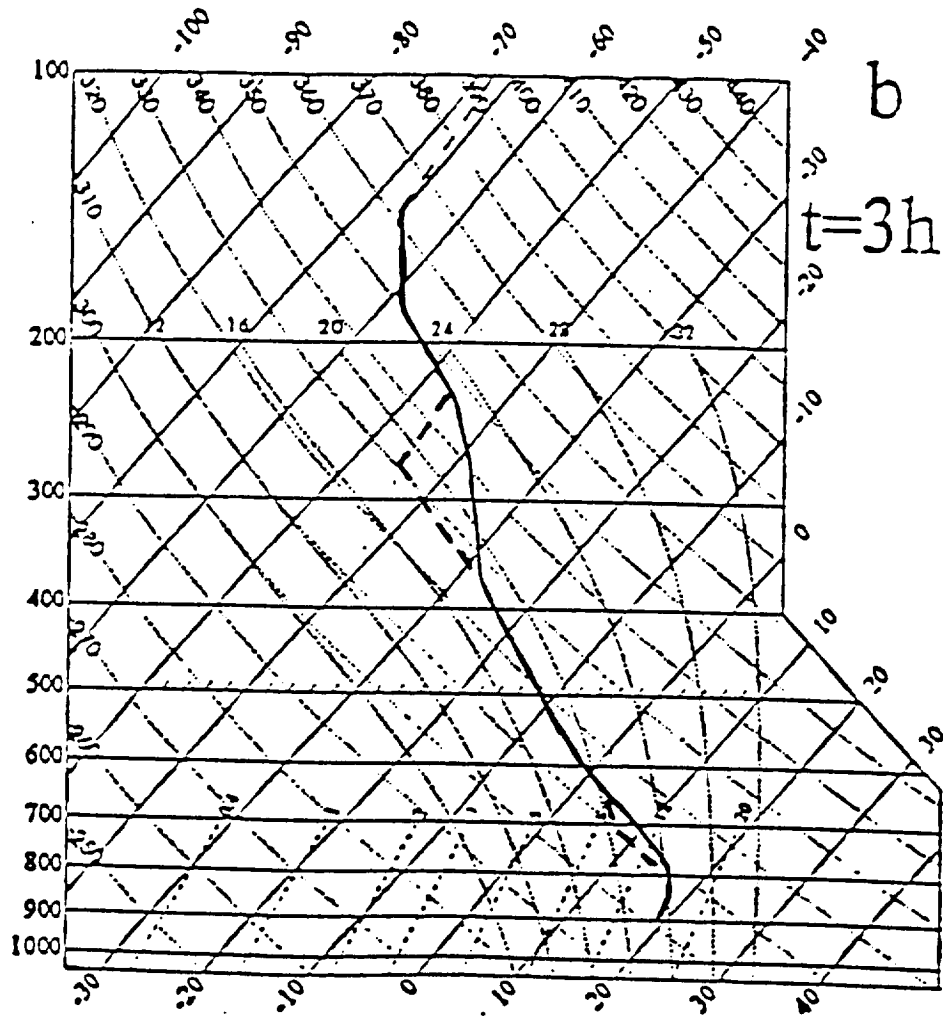


Fig. 1b. The same environment after 3 h of lifting at the rate indicated by Fig. 3 and with imposed low-level cooling (from Kain and Fritsch, 1997)

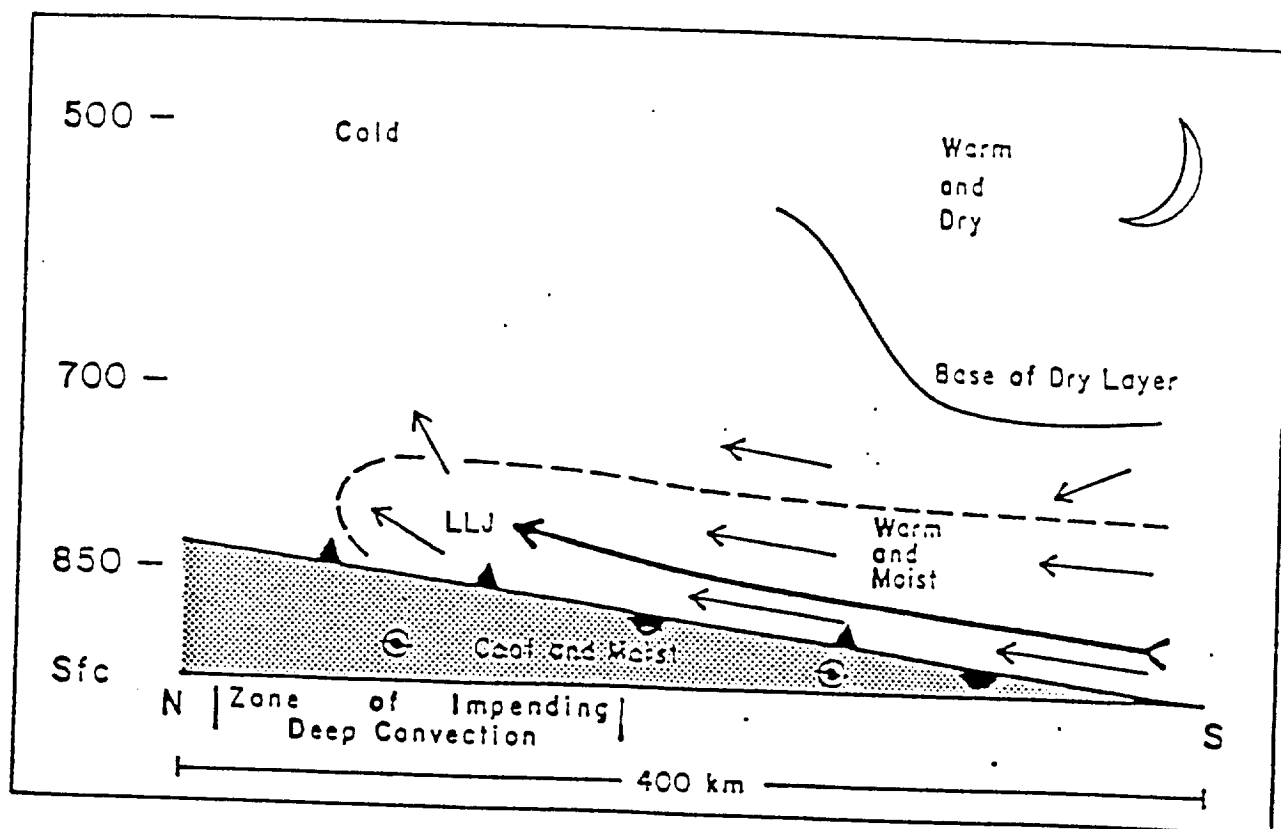


Fig. 2. Conceptual diagram of a low-level jet of warm, moist air overrunning the relatively cool low-level air north of a warm front (from Trier and Parsons, 1993)

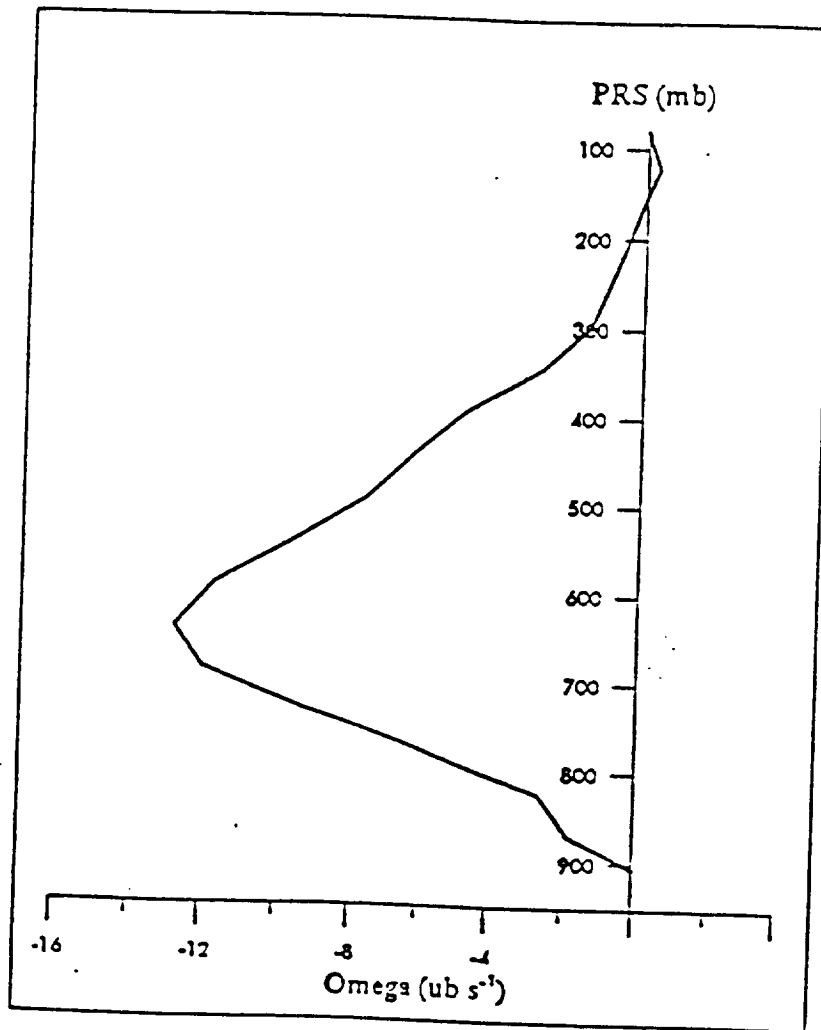


Fig. 3. Vertical profile of vertical motion ($\mu\text{b s}^{-1}$) used to calculate the effects of forced ascent on the sounding shown in Fig. 1a (from Kain and Fritsch, 1997)

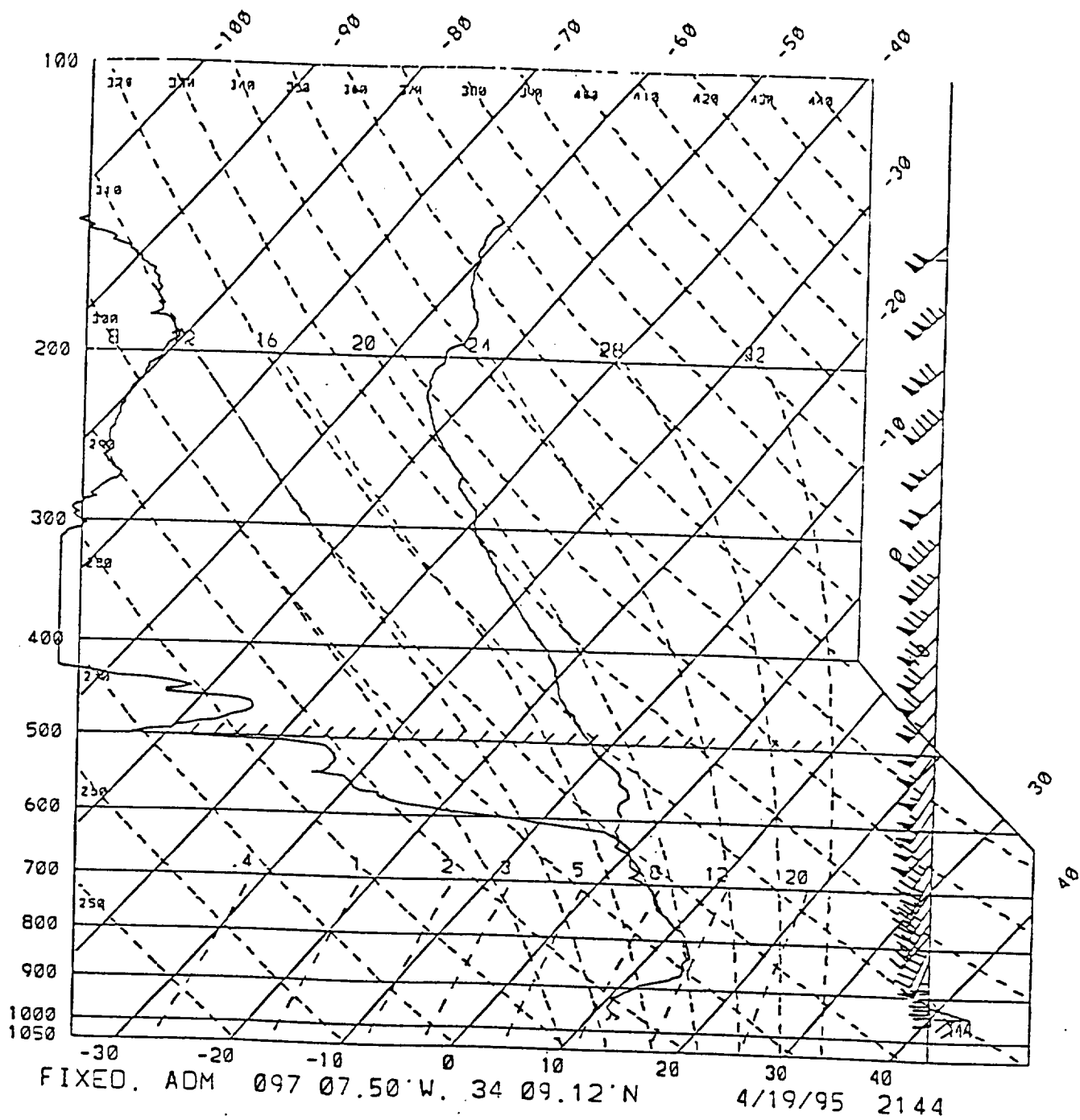


Fig. 4. Vertical sounding derived from radiosonde measurements from Ardmore, OK, valid 2315 UTC 19 April 1995 and plotted on a Skew-T log-P diagram (from Kain and Fritsch, 1997)

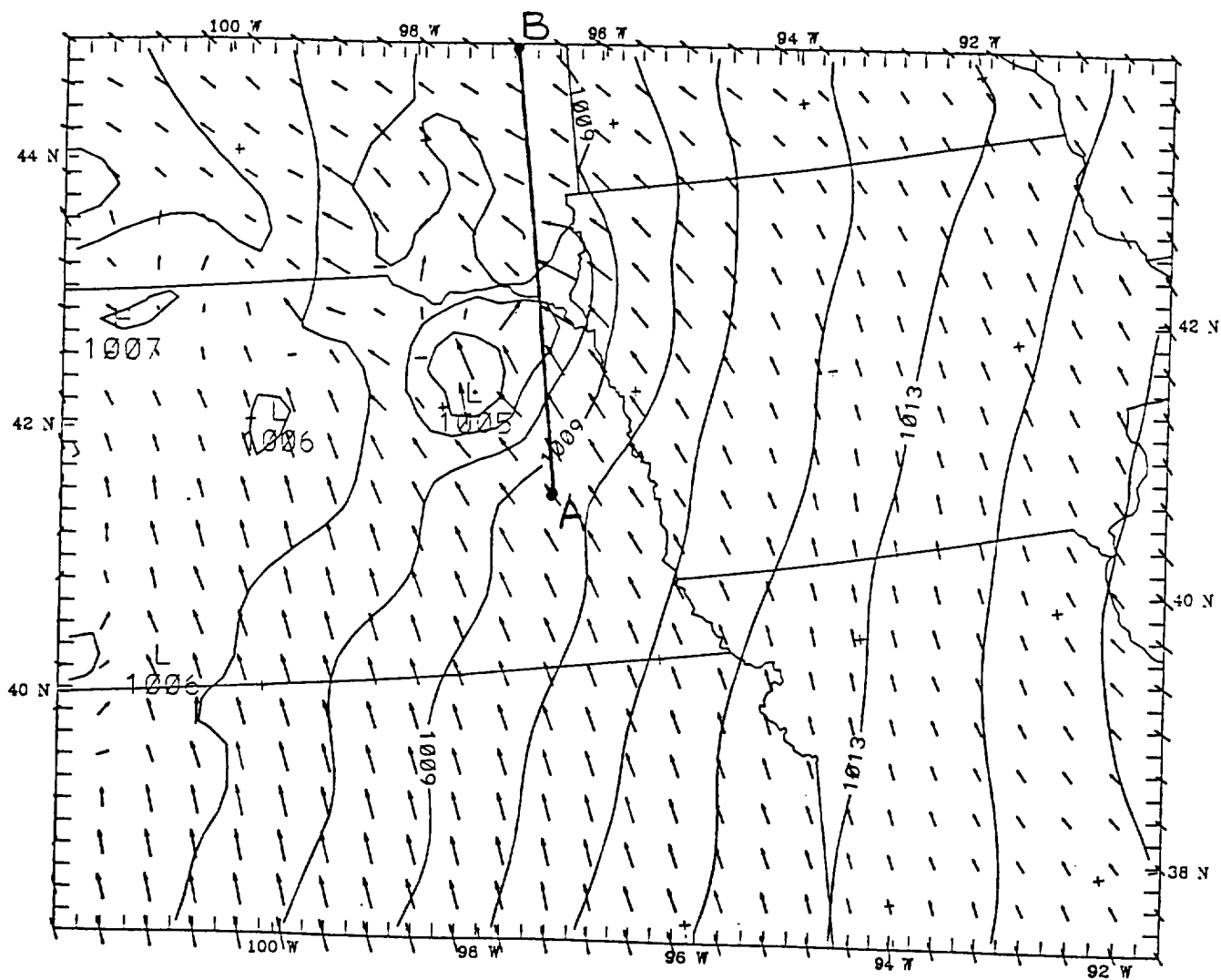
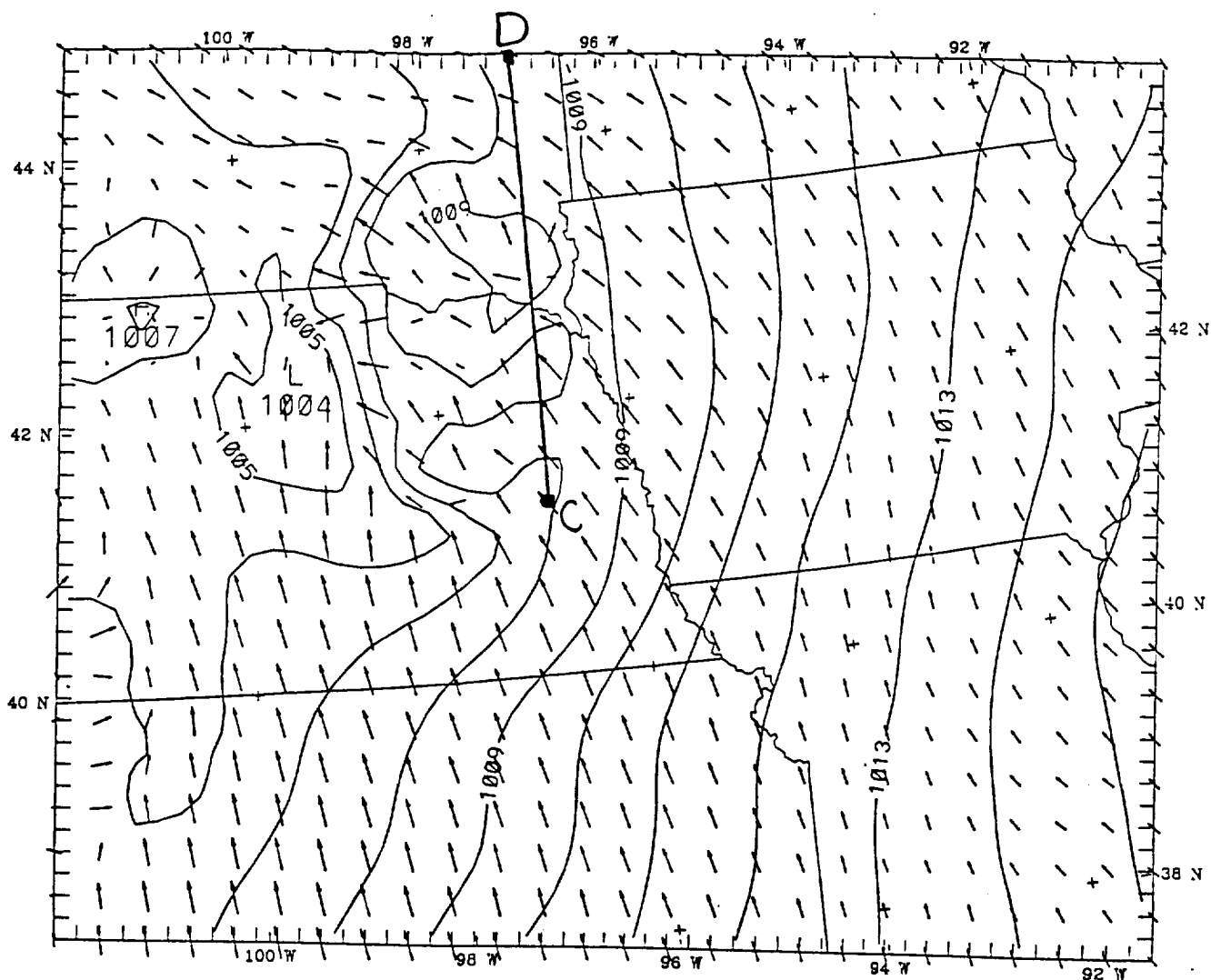


Fig. 5. Sea level pressure (mb) and lowest sigma-level ($\sigma = 0.997$) winds (max vector = 13.5 m s^{-1}) at 15 h for simulation without hybrid procedure. Location of cross sections appearing in Fig. 6 is indicated by line AB.



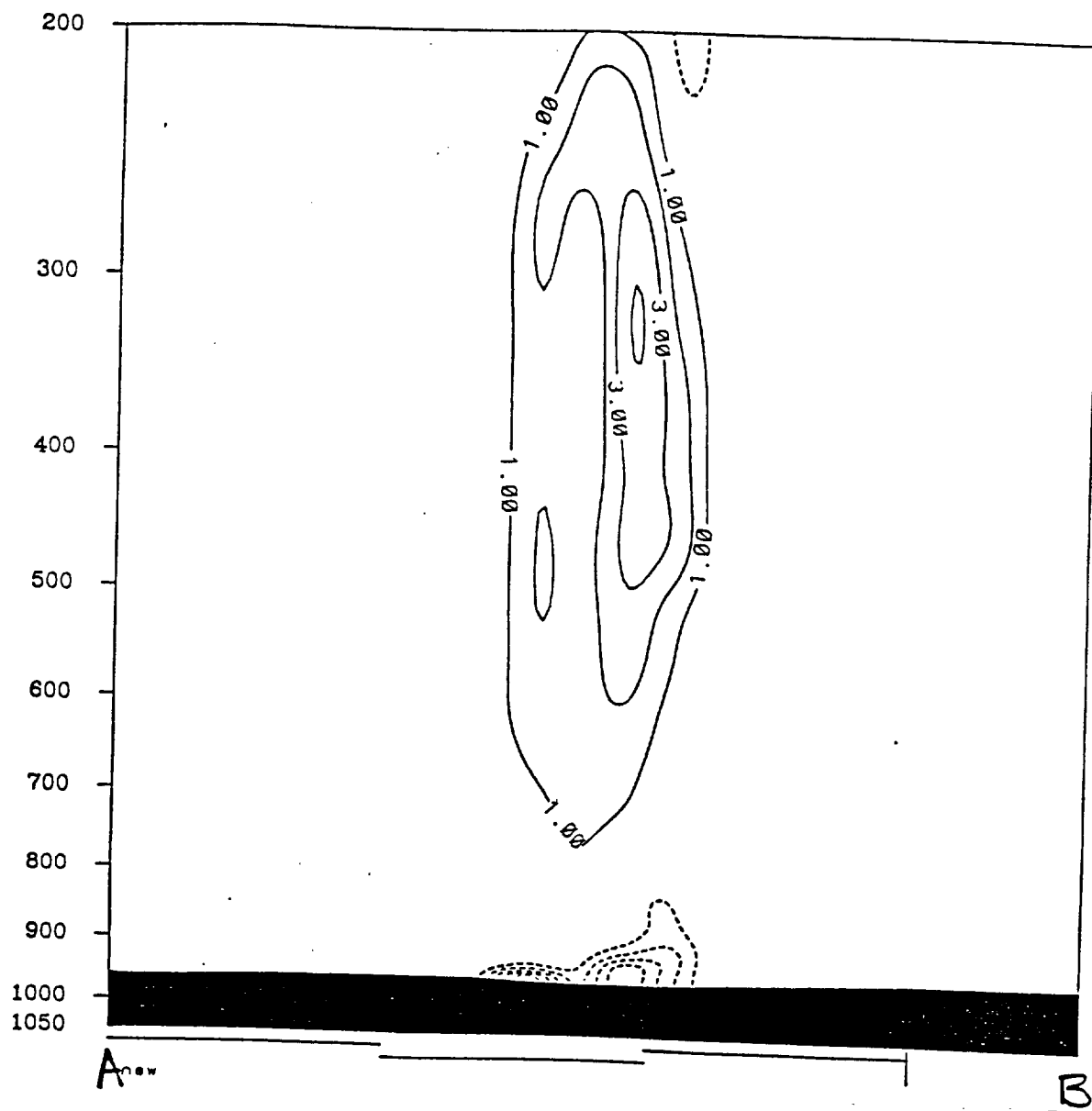


Fig. 7a. Cross section of convective heating at 15 hours from KF convective scheme (K hr^{-1} , contour interval 1 K hr^{-1}) for simulation without hybrid procedure

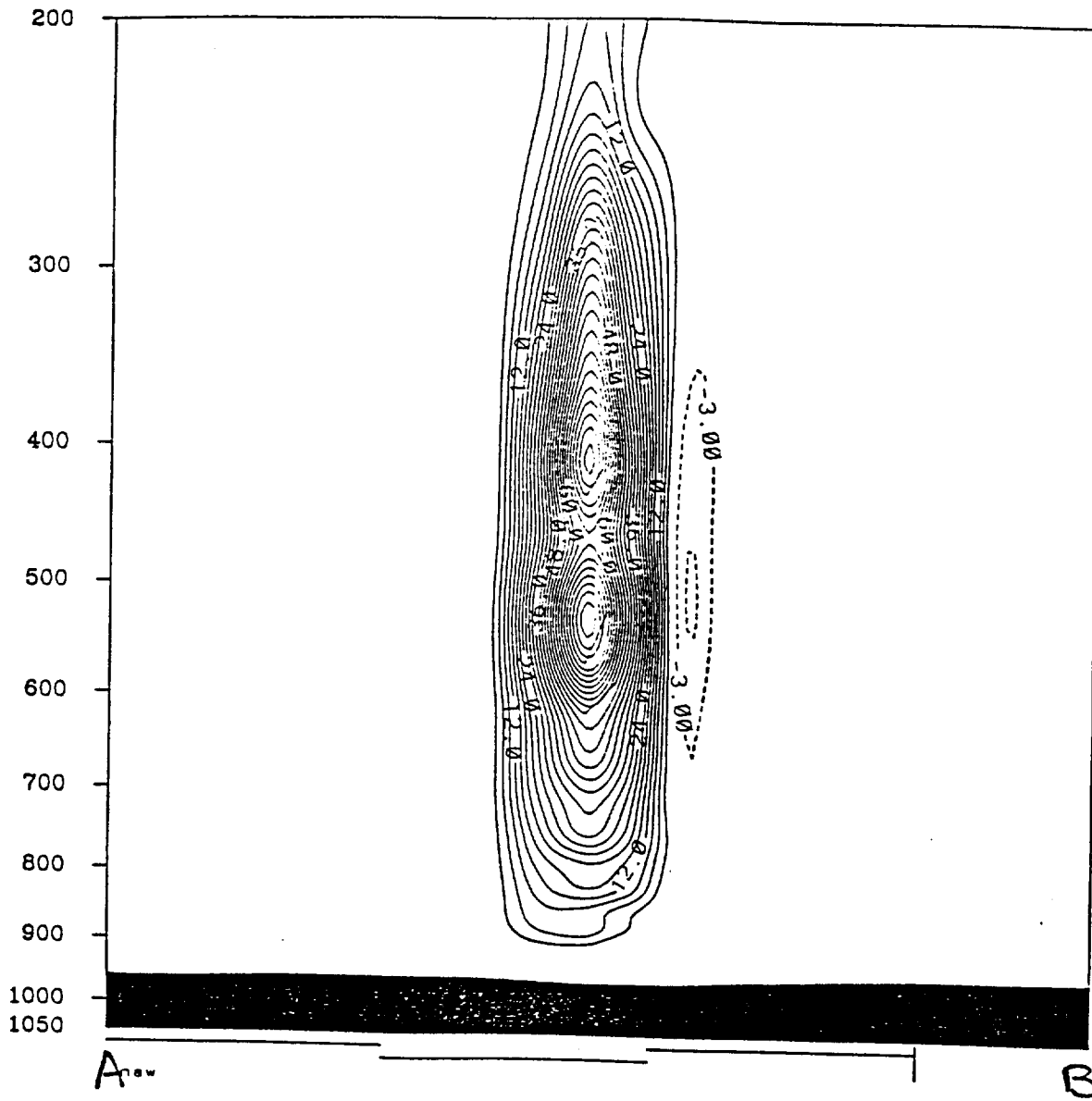


Fig. 7b. Cross section of convective heating at 15 hours from grid scale (K hr^{-1} , contour interval 3 K hr^{-1}) for simulation without hybrid procedure

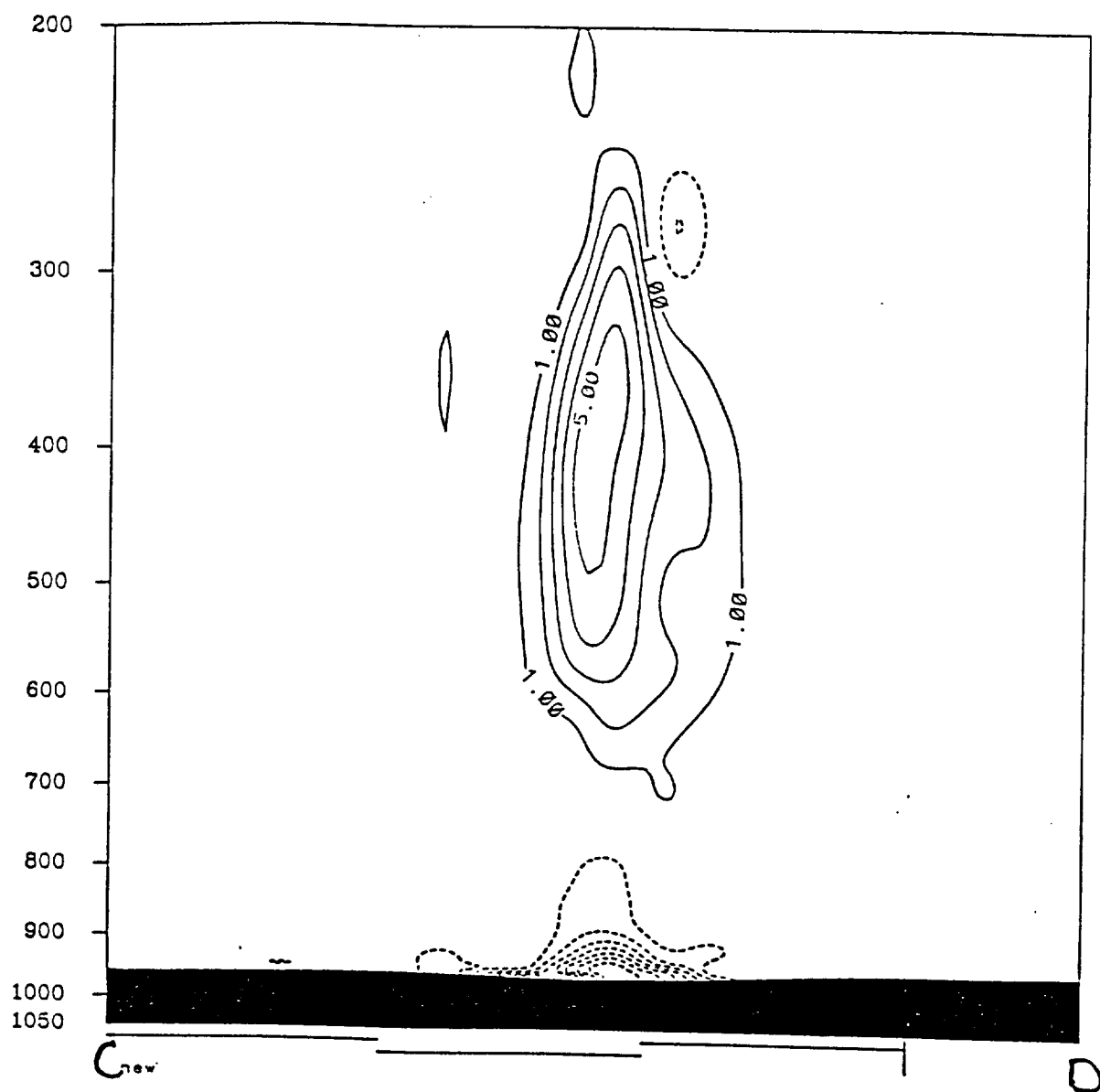


Fig. 8a. As in Fig. 7a, but for simulation with hybrid procedure

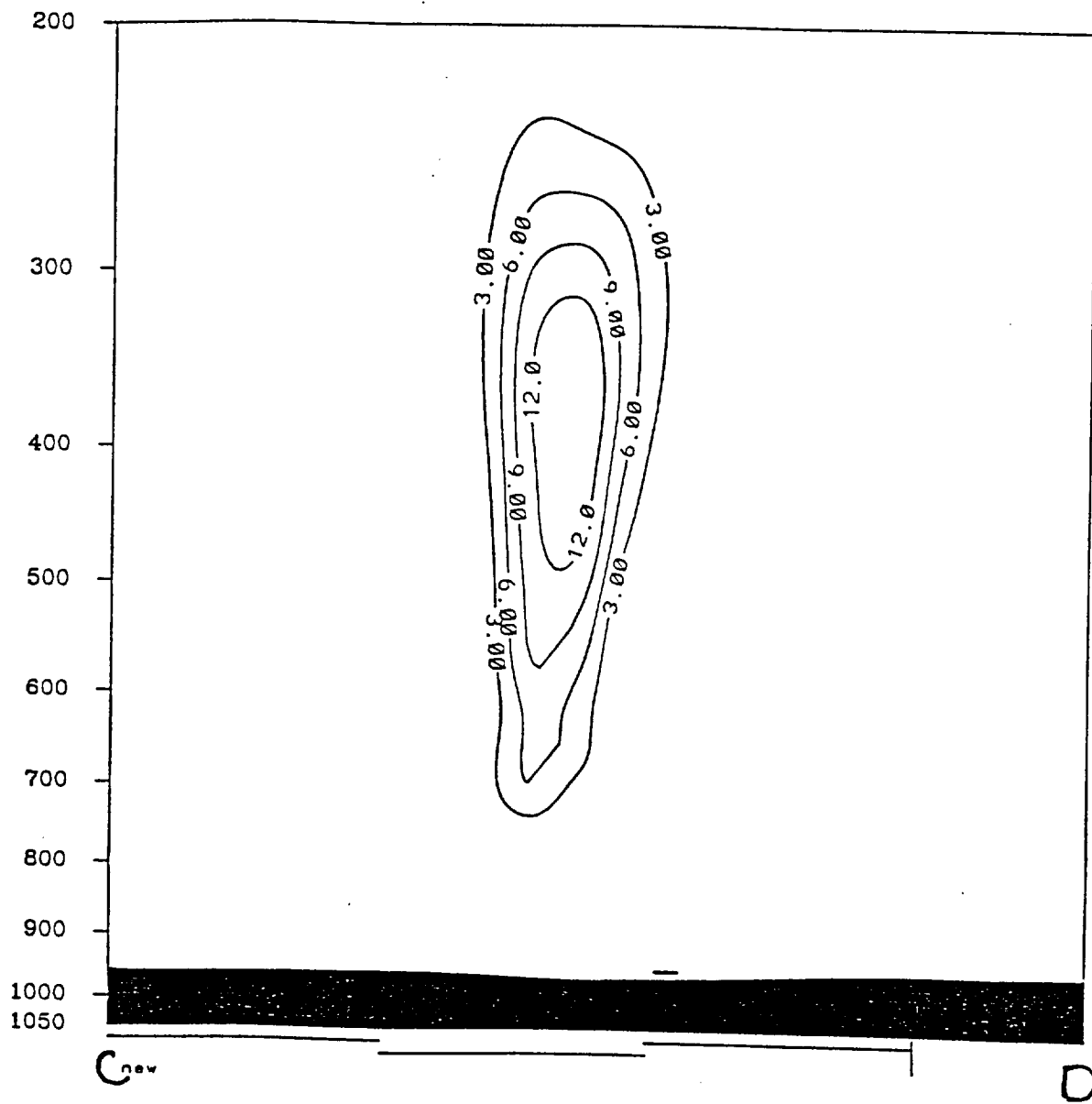


Fig. 8b. As in Fig. 7b, but for simulation with hybrid procedure

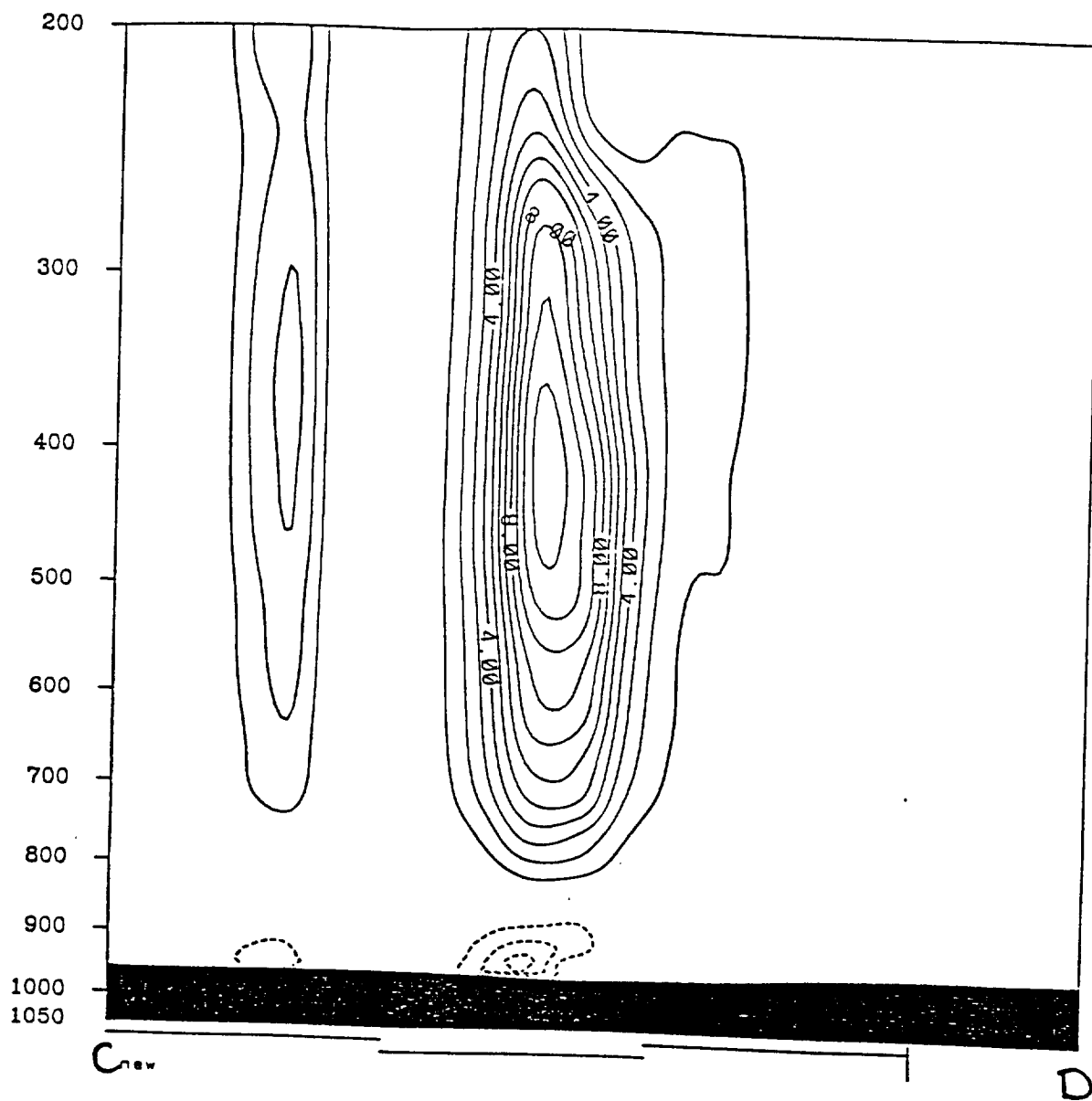


Fig. 8c. Cross section of convective heating at 15 hours from BM convective scheme (K hr^{-1} , contour interval 1 K hr^{-1}) for simulation with hybrid procedure

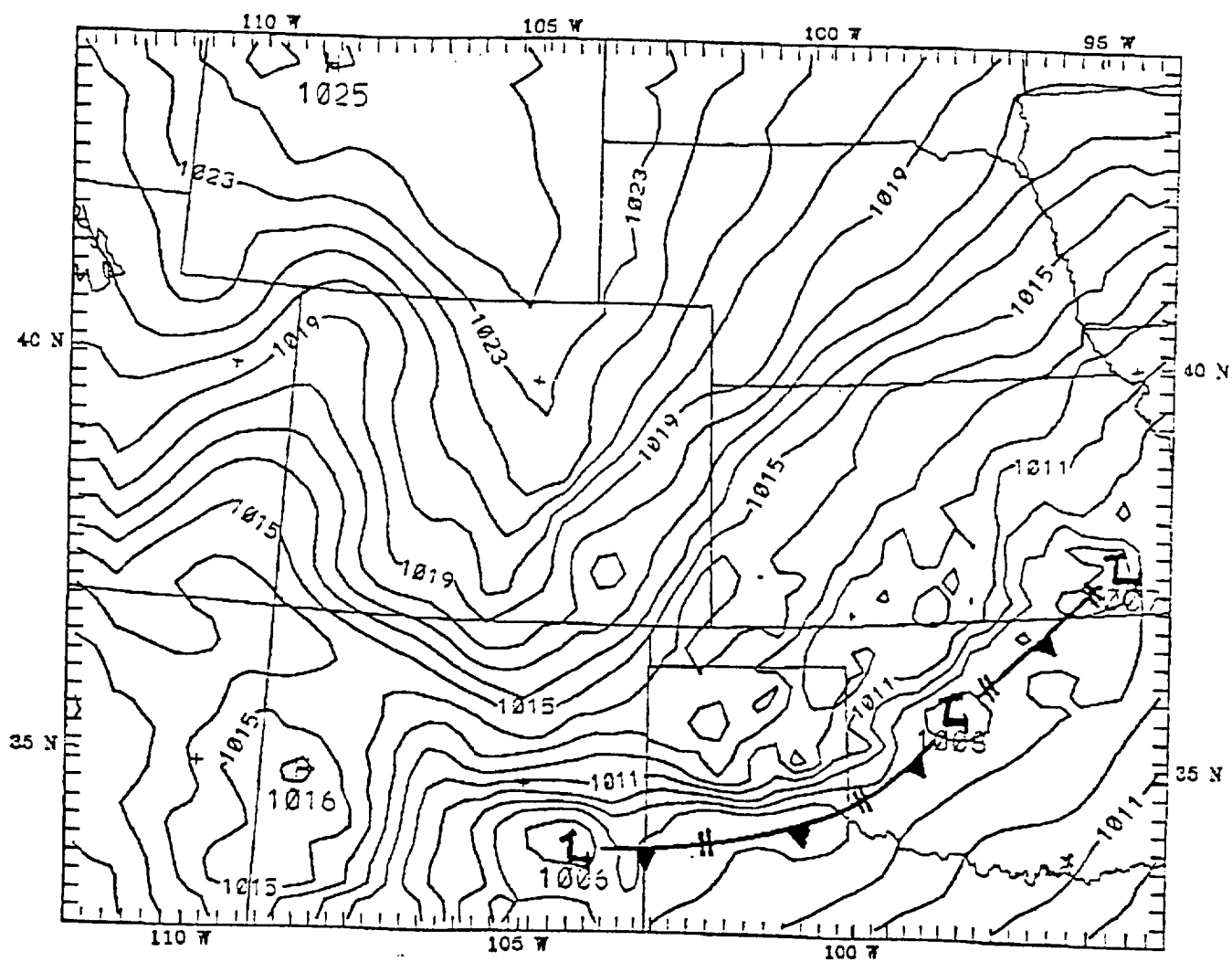


Fig. 9a. Sea-level pressure (mb) at 18 h into a simulation using the mass source/sink type of feedback in the KF scheme

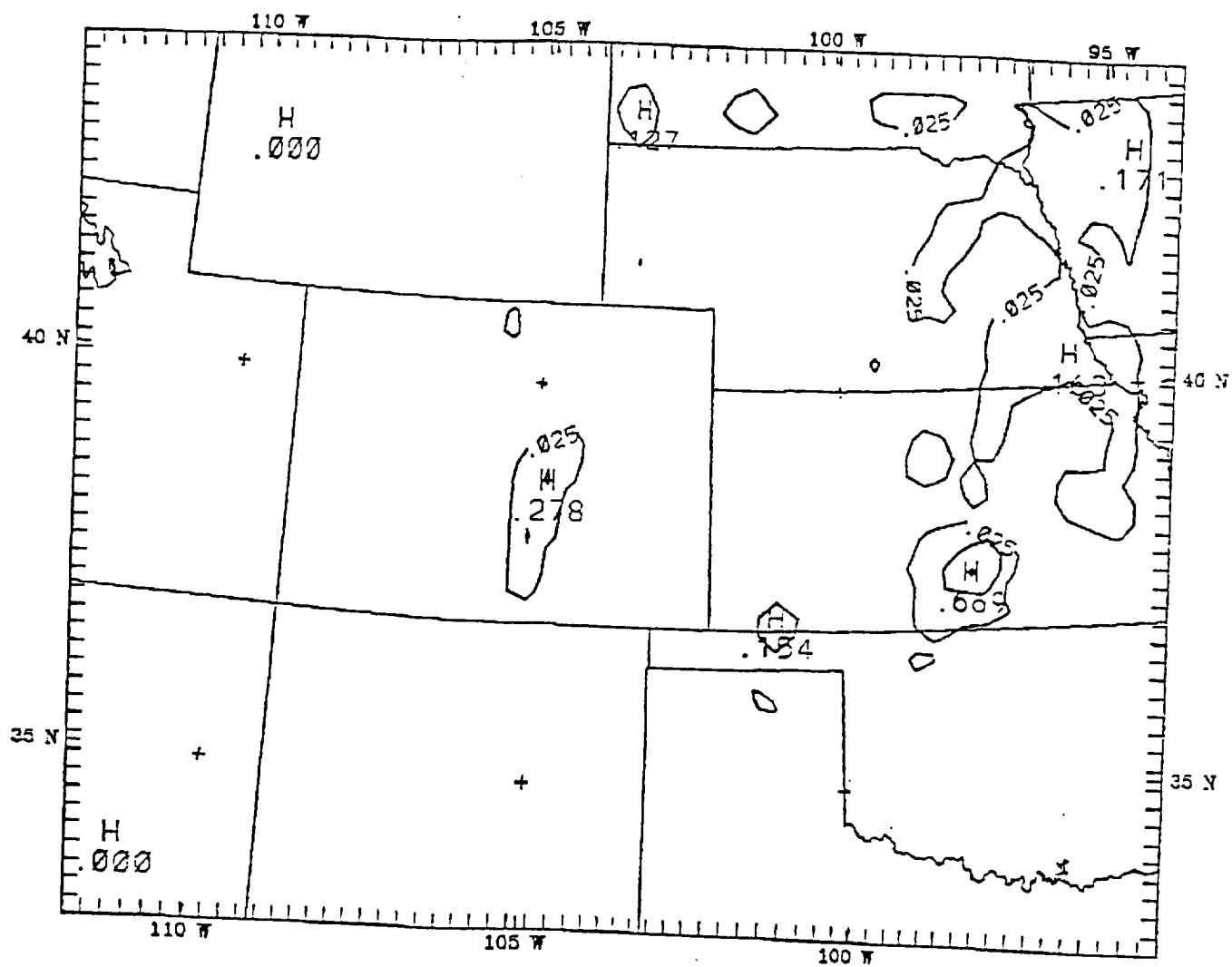


Fig. 9b. Grid-resolved 17 to 18 h rainfall (cm) from a simulation using the mass source/sink type of feedback in the KF scheme:

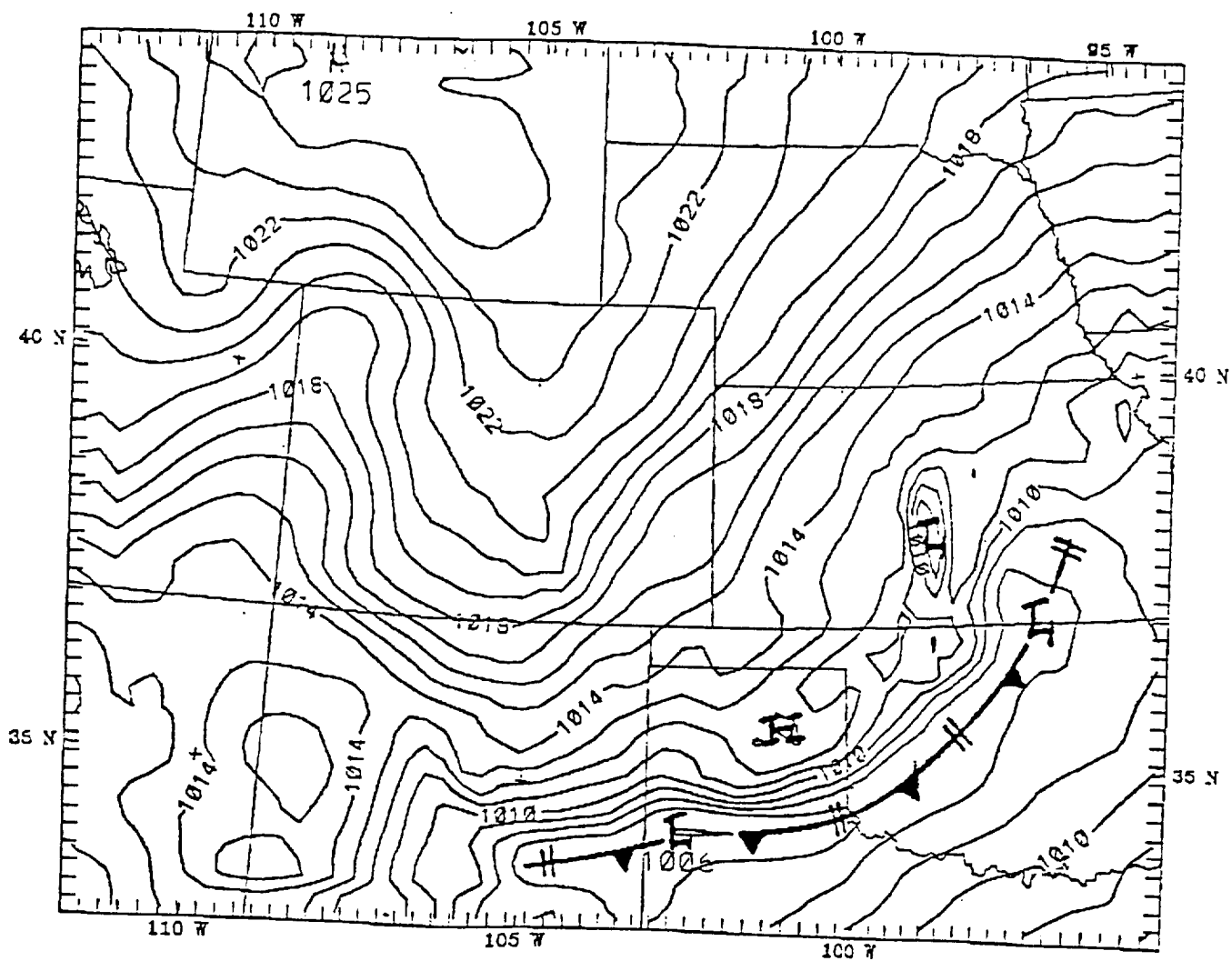


Fig. 10a. As in Fig. 9a, but for a simulation using the normal feedback method in the KF scheme.

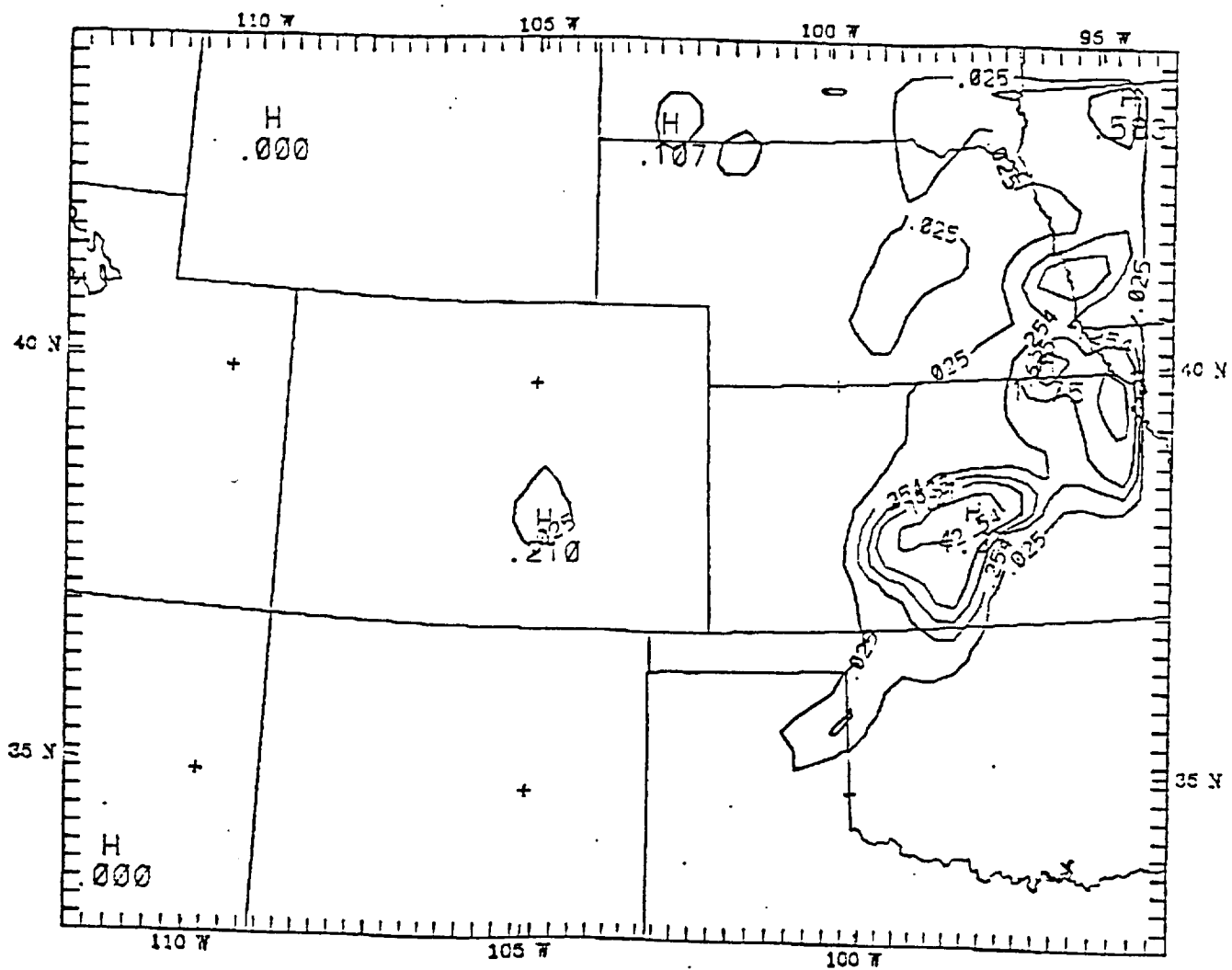


Fig. 10b. As in Fig. 9b, but for a simulation using the normal feedback method in the KF scheme.

Earth and Mineral Sciences/The Pennsylvania State University

Evaluating and Understanding Parameterized Convective Processes and Their
Role in the Development of Mesoscale Precipitation Systems

NASA

Project Dates: 03/01/1997 - 02/28/1998

	03/01/1997 02/28/1998
DIRECT COSTS	
Salaries (Category I)	
J. M. Fritsch	No Charge
Facilities Assistant	575
2% of time	
Staff Assistant	1,417
5% of time	
Subtotal	<u>1,992</u>
Salaries (Category II)	
Graduate Assistant	12,093
50% of time/Grade 18	
Summer & Fall	
Subtotal	<u>12,093</u>
Salaries (Category III)	
Wage Payroll	<u>5,000</u>
Subtotal	<u>5,000</u>
Total Salaries and Wages	19,085
Publications and Page Charges	410
including photocopying	
Maintenance of Equipment	500
including maint contracts	
Fringe Benefits	2,366
refer to Budget Notes	
Total Modified Direct Costs	<u>22,361</u>
Graduate Assistant Tuition	1,490
refer to Budgets Notes	
Total Direct Costs	<u>23,851</u>
INDIRECT COSTS	
Indirect Costs	9,313
refer to budget notes	
TOTAL PROJECT COSTS	<u>\$ 33,164</u>

Proposal number 18-97-1300 - Year 1 indirect cost rate 41.65%; Year 1 fringe rates 26.65%, 11.71%, 8.37%
Cost Proposal System - Version 2.31 02/27/1997 1:20 pm